ChemComm

Synthesis and Optical Properties of Ordered-Vacancy Perovskite Cesium Bismuth Halide Nanocrystals

Journal:	*ChemComm*
Manuscript ID	CC-COM-09-2017-007223.R2
Article Type:	Communication

ChemComm

COMMUNICATION

Synthesis and Optical Properties of Ordered-Vacancy Perovskite Cesium Bismuth Halide Nanocrystals

Received 00th January 20xx,
Accepted 00th January 20xx

DOI: 10.1039/x0xx00000x

www.rsc.org/

R. D. Nelson,[a] K. Santra,[b] Y. Wang,[a] A. Hadi,[a] J.W. Petrich,[b] M.G. Panthani*[a]

Perovskite-phase cesium bismuth halide ($Cs_3Bi_2X_9$; X= Cl, Br, I) nanocrystals were synthesized using a hot-injection approach. These nanocrystals adopted ordered-vacancy perovskite crystal structures and demonstrated composition-tunable optical properties. Growth occurred by initial formation of Bi^0 seeds, and morphology was controlled by precursor and seed concentration. The $Cs_3Bi_2I_9$ nanocrystals demonstrated excellent stability under ambient conditions for several months. Contrary to previous reports, we find that photoluminescence originates from the precursor material as opposed to the perovskite nanocrystals.

Halide perovskite compounds have generated interest as semiconductors with widely tunable properties that are compatible with inexpensive processing methods. The unique properties of halide perovskites show great potential for use in optoelectronic applications like photovoltaics (PVs). Halide perovskite materials typically have the general structure ABX_3, with A as a cation ($CH_3NH_3^+$, $HC(NH_2)_2^+$, Cs^+), B as a metal (Pb, Sn), and X as an anion (Cl^-, Br-,I^-). From ~3.8% efficiency in 2009,[1] the performance of methylammonium lead iodide (MAPbI)-based solar cells has increased rapidly to power conversion efficiencies (PCE) of over 22% in 2017.[2-9] MAPbI has several properties that contribute to this high performance in PVs – a direct bandgap of ~1.5 eV, long charge carrier diffusion lengths, high defect-tolerance, and small exciton binding energies.[10-16] However, stability and toxicity remain an issue for MAPbI and related halide perovskite semiconductors.[17, 18] It is well-known that exposure to moderate humidity, temperatures, or insolation can degrade MAPbI.[19-23]

Attempts to improve stability of halide perovskite PVs have typically involved partial or full substitution of the A-site cation and X-site anion. [2, 24-30] Using colloidal halide perovskite nanocrystals (NCs) can also enhance stability.[31] Swarnkar et al. processed halide perovskite NCs into thin films with enhanced stability.[32] Perovskite $CsPbI_3$ NCs adopt the black cubic perovskite phase (α-$CsPbI_3$), which is thermodynamically unstable at room temperature in the bulk.[33] The enhanced stability of the α-phase has been attributed to surface stabilization by the cationic ligands,[34] though the NCs can eventually revert back to the yellow non-perovskite δ-phase[35] which has poor optoelectronic properties.

In addition to addressing stability, there have been efforts to develop Pb-free halide perovskites. Alternatives to Pb include other $6s^2$ elements such as antimony and bismuth. Recently, bismuth halides and oxyhalides[36,37] have demonstrated promise as PV materials, aided by the soft polarizability and defect tolerance of bismuth.[38] Initial PV devices with BiI_3 as the active layer possessed a PCE of 1%.[36] Bismuth has also been incorporated into defect perovskites with formula $A_3B_2X_9$. $Cs_3Bi_2I_9$ films in hexagonal phase were incorporated into ~1% efficient solar cells.[39] NCs of bismuth based halides have been synthesized via room-temperature reaction[40,41] and hot-injection.[42] Work has also been done on synthesizing antimony halide NCs,[43] showing promising photoluminescence quantum yield.[44] In general, there is much promise for lead free halide NCs,[45] motivating research into growth mechanisms to further enhance efforts to optimize these materials.

Given the feasibility of synthesizing cesium bismuth halide NCs, we investigated the hot-injection synthesis of $Cs_3Bi_2X_9$ NCs, where X includes Cl, Br, and I, in order to elucidate the growth mechanism. To synthesize $Cs_3Bi_2X_9$ NCs, we initially adapted the method for synthesizing $CsPbI_3$ NCs developed Protesescu et al.,[33] with modifications to the precursor stoichiometry (see ESI for details). In a typical reaction, heated Cs-oleate was injected into a heated mixture of bismuth halide salt, ODE, OA, and oleylamine (OLA). To quench reactions, room-temperature toluene was injected directly into the crude reaction mixture while stirring. To avoid degradation, the NCs were precipitated by simply centrifuging the NCs (see ESI for details).

[a] Department of Chemical and Biological Engineering, Iowa State University, Ames, IA 50011, *Email: panthani@iastate
[b] Department of Chemistry, Iowa State University, Ames, IA 50011
[c] U.S. Department of Energy, Ames Laboratory, Ames, IA 50011
Electronic Supplementary Information (ESI) available: Experimental details, Figures S1-S7. See DOI: 10.1039/x0xx00000x

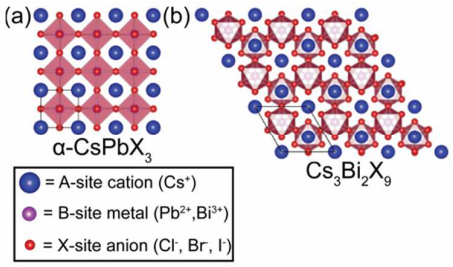

Figure 1. Illustrations depicting the crystal structures of (a) the conventional, ABX_3 cubic perovskite (**α -$CsPbI_3$-type**) and (b) the ordered-vacancy perovskite structure adopted by $Cs_3Bi_2X_9$. Both are viewed down the c-axis. Designed using VESTA.[46]

Bulk $Cs_3Bi_2X_9$ is known to adopt an ordered-vacancy perovskite structure[47] (Fig. 1b). The cubic ABX_3 perovskite (Fig. 1a) has corner-sharing octahedra of PbX_6, with the A-site cations in the cuboctahedral voids. The $A_3Bi_2X_9$ structure, in contrast, has pairs of face-sharing BiX_6 octahedra which form $Bi_2X_9^{3-}$ dimer-like units. These double octahedron are surrounded by the A-site cations. X-ray diffraction (XRD) of $Cs_3Bi_2I_9$ NCs powders confirmed that the NCs synthesized here had this structure (Fig. 2a). The prominence of the (006) reflection compared to the (203), (204), and (205) reflections suggests that the nanocrystals grow anisotropically, with preferential growth along the c-axis.

Transmission electron microscopy (TEM) shows that $Cs_3Bi_2I_9$ NCs are faceted and polydisperse (39.5 ± 9.3 nm diameter) with regards to crystallite size (Fig. 2b). High-resolution TEM (HRTEM) confirms that the $Cs_3Bi_2I_9$ NCs are single crystals with an ordered defect perovskite structure (Fig. 2c). In many TEM images of $Cs_3Bi_2X_9$ NCs, we observed the presence of small (< 3 nm) particles; the lattice of these particles could not be resolved. We found that these small particles are formed in the BiI_3/OA/OLA reaction precursor (Fig. 3a) before injecting Cs-oleate. This implies that these particles could be Bi^0 seeds that form during the dissolution of BiI_3. This is consistent with previous reports,[48] where Pb^0

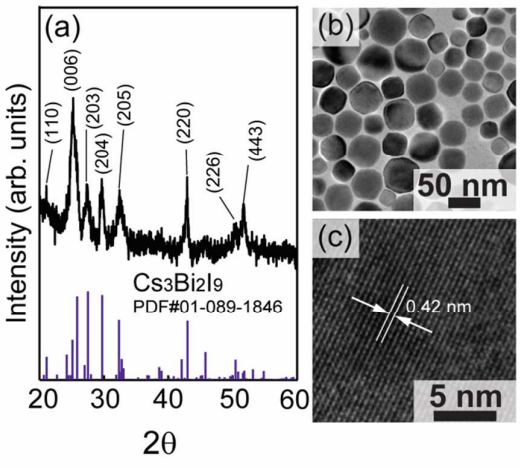

Figure 2. (a) XRD patterns, (b) TEM and (c) HRTEM images of $Cs_3Bi_2I_9$. Pattern for bulk $Cs_3Bi_2I_9$ is included for reference.

seeds were found to form after the dissolution of PbI_2 in a mixture of ODE, OA, and OLA. We hypothesize that these Bi^0 seeds then react with injected Cs-oleate, with some control of growth afforded by variation in reactant concentration and additional ligands.

The $Cs_3Bi_2I_9$ NC morphology was found to be sensitive to the ratio and concentration of Bi and Cs precursors used during synthesis. When using a near stoichiometric concentration of BiI_3 and Cs-oleate ~40 nm quasi-spherical NCs were formed (Fig. 3b). In this case, the reaction occurs under conditions of slight excess of Cs-oleate, possibly indicating that excess oleic acid ligands or Cs-oleate will facilitate the growth of spherical NCs over the more faceted NCs. This type of effect has been observed before – previous reports have demonstrated that the morphology of metal and metal chalcogenide NCs can be tuned by adjusting the concentration of alkali metal oleate precursor used during synthesis.[49, 50] We found that reducing the amount of BiI_3 precursor results in a lower concentration of Bi^0 nuclei, which could impact the growth and resulting size of the NCs, consistent with a previous report that found precursor concentration for $Cs_3Bi_2X_9$ had an impact on resulting NC size.[41] Using four times excess of BiI_3 resulted in more faceted particles with higher polydispersity and the ubiquitous appearance of Bi^0 metal seeds. In contrast, when an eight times excess of BiI_3 was used, no additional change in the $Cs_3Bi_2I_9$ NC morphology was observed (Fig. 3d). However, there was a larger concentration of small seed-like particles, supporting the proposed mechanism of formation of Bi^0 seeds.

These results imply that the growth of the $Cs_3Bi_2X_9$ NCs is initiated by the number of Bi^0 nuclei; we hypothesize further control over size and morphology could be obtained by controlling the number of these nuclei in solution. In support of this hypothesis, we found that aging the BiI_3/ODE/OA/OLA precursor prior to the injection of Cs-oleate promotes the formation of anisotropic long rectangular NCs (Fig. S2).

The morphology of the $Cs_3Bi_2X_9$ NCs can be further tuned by introducing different capping ligands during synthesis. For example, we found that including trioctylphosphine (TOP) into the precursor mixture resulted in a higher concentration of rectangular NCs (Fig. S1). This could indicate that TOP attaches

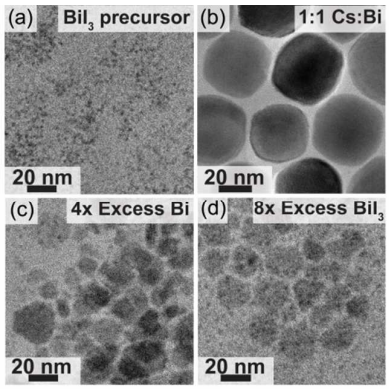

Figure 3. TEM of a) unreacted BiI_3 precursor, (b) reaction at 120°C for 30 seconds, (c) four times the Bi concentration of 3b, and (d) eight times the Bi concentration of 3b.

to specific facets of the $Cs_3Bi_2I_9$ NCs during nucleation and growth. Similar anisotropic growth was reported for $CsPbI_3$ NCs that were synthesized in a reaction mixture containing polar molecules.[48] Udayabhaskararao et al.[48] deduced that the polar environment in the $CsPbI_3$ NC reaction mixture facilitated amine protonation, with ammonium species acting to passivate surfaces[51] and preferentially bind to replace the Cs^+ ions. It is possible that a similar mechanism could explain our observed morphology when adding TOP, which is moderately polar. However, given that aging the TOP-free precursor also results in the appearance of long rectangular nanostructures (Fig. S2) and considering that TOP is a reducing agent, adding TOP to the reaction mixture may accelerate the formation of Bi^0 seeds, simulating what would occur in an "aged" precursor.

We found that changing the reaction temperature had little effect on the size or shape of the $Cs_3Bi_2I_9$ NCs (Fig. S3). Increasing reaction time resulted in a relatively small increase in particle size. Based on our studies of reaction time, it appears that the NC size and shape are rapidly defined within the first few seconds of reaction (Fig. S4).

The $Cs_3Bi_2I_9$ NCs demonstrate remarkable stability under ambient storage conditions for long periods of time. The characteristic absorbance peak at 489 nm remains unchanged for at least 100 days when stored in a vial outside the glovebox after exposure to ambient conditions and the XRD pattern matches to the $Cs_3Bi_2I_9$ reference (Fig. S5). In contrast $CsPbI_3$ NCs have been reported to degrade in a few days once exposed to air.[48] This stability makes $Cs_3Bi_2I_9$ NCs promising for incorporation into highly stable optoelectronic devices.

The synthesis method could be extended to other halides (TEM shown in Fig S6) by using different BiX_3 salts. $Cs_3Bi_2Br_9$ NCs exhibited a similar morphology to $Cs_3Bi_2I_9$, but the $Cs_3Bi_2Cl_9$ NCs formed rectangular nanoplatelets. It was observed that the $Cs_3Bi_2I_9$ had the fewest number of Bi^0 seeds at concentrations equivalent to the other halides – this may be due to solubility differences between the BiX_3 salts. The BiI_3 was the most readily soluble. By varying composition, the absorbance maximum of the $Cs_3Bi_2X_9$ NCs (where X indicates either single- or mixtures of halides) could be tuned between 331 (X = Cl) and 489 nm (X = I) as seen in Fig. S7a.

We noticed that mixed halide NCs (X= Br, I or Br, Cl) had broader absorption peaks compared to single-halide NCs. This implies that the mixed-halide NCs may be a mixture of single-halide NCs rather than mixed-halide alloy NCs; however, in TEM only a single morphology is observed (Fig. S7b and S7c). This behaviour is markedly different than $CsPbX_3$ NCs, which are known to readily exchange halides even with other halide-containing NCs in colloidal dispersions.[52,53] The apparent inability to synthesize mixed-halide $Cs_3Bi_2X_9$ NCs could be explained by differences in mobility of anions in the defect perovskite structure, differences in B-X bond energies, or differences in precursor decomposition kinetics.

The measurement and investigation of PL properties and improvement of PL quantum yield is the subject of ongoing research, with the expectation that the predicted excellent defect-tolerance of $Cs_3Bi_2X_9$[54] should result in easily detectable

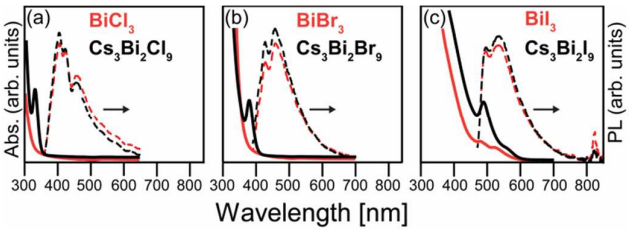

Figure 4. Absorbance (solid) and photoluminescence (dashed) spectra for $Cs_3Bi_2X_9$ NCs of X = (a) Cl; (b) Br; (c) I

PL with decent PL quantum yield. However, initial results have shown that PL observed in the reaction products is also found in the reaction precursor prior to injection of Cs-oleate (Fig. 4). While similar trends in PL have been reported in other manuscripts[40,41,42] the true origin of this PL is unclear, given the difficulty in separating the precursor material from the resulting nanoparticles via centrifugation and the lack of analysis of the precursors in the aforementioned literature.

In conclusion, we report the synthesis of $Cs_3Bi_2X_9$ NCs with an ordered-vacancy halide perovskite composition, identified factors that influence size and morphology, and characterized their composition-tunable optical properties. The growth mechanism was found to have similarities to that of $CsPbI_3$ NCs, where growth is initiated by Bi^0 metal seeds that subsequently react with injected Cs-oleate. The widely-tunable absorbance and air stability of these $Cs_3Bi_2X_9$ NCs shows an important step toward stable and efficient Pb-free perovskite optoelectronic devices.

This material is based upon work supported by the National Science Foundation Graduate Research Fellowship Program under Grant No. (DGE1247194). Any opinions, findings, and conclusions or recommendations expressed in this material are those of the author(s) and do not necessarily reflect the views of the National Science Foundation. JWP was supported by the U.S. Department of Energy, Office of Basic Energy Sciences, Division of Chemical Sciences, Geosciences, and Biosciences through the Ames Laboratory. The Ames Laboratory is operated for the U.S. Department of Energy by Iowa State University under Contract No. DE-AC02-07CH11358.

Conflicts of Interest

There are no conflicts to declare.

Notes and references

1. A. Kojima, K. Teshima, Y. Shirai and T. Miyasaka, *J. Am. Chem. Soc.*, 2009, 131, 6050-6051.
2. M. Saliba, T. Matsui, J.-Y. Seo, K. Domanski, J.-P. Correa-Baena, M. K. Nazeeruddin, S. M. Zakeeruddin, W. Tress, A. Abate, A. Hagfeldt and M. Gratzel, *Energy Environ. Sci.*, 2016, 9, 1989-1997.
3. NREL, Best Research-Cell Efficiencies, http://www.nrel.gov/ncpv/images/efficiency_chart.jpg
4. N. Ahn, D.-Y. Son, I.-H. Jang, S. M. Kang, M. Choi and N.-G. Park, *J. Am. Chem. Soc.*, 2015, 137, 8696-8699.

5. C.-G. Wu, C.-H. Chiang, Z.-L. Tseng, M. K. Nazeeruddin, A. Hagfeldt and M. Gratzel, *Energy Environ. Sci.*, 2015, 8, 2725-2733.
6. N. J. Jeon, J. H. Noh, W. S. Yang, Y. C. Kim, S. Ryu, J. Seo and S. I. Seok, *Nature*, 2015, 517, 476-480.
7. M. M. Lee, J. Teuscher, T. Miyasaka, T. N. Murakami and H. J. Snaith, *Science*, 2012, 338, 643.
8. M. Liu, M. B. Johnston and H. J. Snaith, *Nature*, 2013, 501, 395-398.
9. J. Burschka, N. Pellet, S.-J. Moon, R. Humphry-Baker, P. Gao, M. K. Nazeeruddin and M. Gratzel, *Nature*, 2013, 499, 316-319.
10. S. D. Stranks, G. E. Eperon, G. Grancini, C. Menelaou, M. J. P. Alcocer, T. Leijtens, L. M. Herz, A. Petrozza and H. J. Snaith, *Science*, 2013, 342, 341.
11. D. Shi, V. Adinolfi, R. Comin, M. Yuan, E. Alarousu, A. Buin, Y. Chen, S. Hoogland, A. Rothenberger, K. Katsiev, Y. Losovyj, X. Zhang, P. A. Dowben, O. F. Mohammed, E. H. Sargent and O. M. Bakr, *Science*, 2015, 347, 519.
12. G. Xing, N. Mathews, S. Sun, S. S. Lim, Y. M. Lam, M. Grätzel, S. Mhaisalkar and T. C. Sum, *Science*, 2013, 342, 344.
13. M. A. Green, A. Ho-Baillie and H. J. Snaith, *Nat. Photon.*, 2014, 8, 506-514.
14. S. De Wolf, J. Holovsky, S.-J. Moon, P. Löper, B. Niesen, M. Ledinsky, F.-J. Haug, J.-H. Yum and C. Ballif, *J. Phys. Chem. Lett.*, 2014, 5, 1035-1039.
15. L. M. Pazos-Outón, M. Szumilo, R. Lamboll, J. M. Richter, M. Crespo-Quesada, M. Abdi-Jalebi, H. J. Beeson, M. Vrućinić, M. Alsari, H. J. Snaith, B. Ehrler, R. H. Friend and F. Deschler, *Science*, 2016, 351, 1430.
16. M. I. Saidaminov, A. L. Abdelhady, B. Murali, E. Alarousu, V. M. Burlakov, W. Peng, I. Dursun, L. Wang, Y. He, G. Maculan, A. Goriely, T. Wu, O. F. Mohammed and O. M. Bakr, *Nat. Commun.*, 2015, 6, 7586.
17. T. A. Berhe, W.-N. Su, C.-H. Chen, C.-J. Pan, J.-H. Cheng, H.-M. Chen, M.-C. Tsai, L.-Y. Chen, A. A. Dubale and B.-J. Hwang, *Energy Environ. Sci.*, 2016, 9, 323-356.
18. S. D. Stranks and H. J. Snaith, *Nat. Nanotechnol.*, 2015, 10, 391-402.
19. Y. Han, S. Meyer, Y. Dkhissi, K. Weber, J. M. Pringle, U. Bach, L. Spiccia and Y.-B. Cheng, *J. Mater. Chem. A*, 2015, 3, 8139-8147.
20. R. K. Misra, S. Aharon, B. Li, D. Mogilyansky, I. Visoly-Fisher, L. Etgar and E. A. Katz, *J. Phys. Chem. Lett.*, 2015, 6, 326-330.
21. B. Conings, J. Drijkoningen, N. Gauquelin, A. Babayigit, J. D'Haen, L. D'Olieslaeger, A. Ethirajan, J. Verbeeck, J. Manca, E. Mosconi, F. D. Angelis and H.-G. Boyen, *Adv. Energy Mater.*, 2015, 5, 1500477-n/a.
22. J. Yang, B. D. Siempelkamp, D. Liu and T. L. Kelly, *ACS Nano*, 2015, 9, 1955-1963.
23. B. Hailegnaw, S. Kirmayer, E. Edri, G. Hodes and D. Cahen, *J. Phys. Chem. Lett.*, 2015, 6, 1543-1547.
24. Y. Ogomi, A. Morita, S. Tsukamoto, T. Saitho, N. Fujikawa, Q. Shen, T. Toyoda, K. Yoshino, S. S. Pandey, T. Ma and S. Hayase, *J. Phys. Chem. Lett.*, 2014, 5, 1004-1011.
25. F. Hao, C. C. Stoumpos, R. P. H. Chang and M. G. Kanatzidis, *J. Am. Chem. Soc.*, 2014, 136, 8094-8099.
26. Y. Li, W. Sun, W. Yan, S. Ye, H. Rao, H. Peng, Z. Zhao, Z. Bian, Z. Liu, H. Zhou and C. Huang, *Adv. Energy Mater.,* 2016, 6, 1601353-n/a.
27. J. H. Noh, S. H. Im, J. H. Heo, T. N. Mandal and S. I. Seok, *Nano Lett.*, 2013, 13, 1764-1769.
28. G. E. Eperon, S. D. Stranks, C. Menelaou, M. B. Johnston, L. M. Herz and H. J. Snaith, *Energy Environ. Sci.*, 2014, 7, 982-988.
29. M. Saliba, T. Matsui, K. Domanski, J.-Y. Seo, A. Ummadisingu, S. M. Zakeeruddin, J.-P. Correa-Baena, W. R. Tress, A. Abate, A. Hagfeldt and M. Grätzel, *Science*, 2016, 354, 206.
30. C. Yi, J. Luo, S. Meloni, A. Boziki, N. Ashari-Astani, C. Gratzel, S. M. Zakeeruddin, U. Rothlisberger and M. Gratzel, *Energy Environ. Sci.*, 2016, 9, 656-662.
31. M. C. Weidman, A. J. Goodman and W. A. Tisdale, *Chem. Mater.*, 2017, 29, 5019-5030.
32. A. Swarnkar, A. R. Marshall, E. M. Sanehira, B. D. Chernomordik, D. T. Moore, J. A. Christians, T. Chakrabarti and J. M. Luther, *Science*, 2016, 354, 92.
33. L. Protesescu, S. Yakunin, M. I. Bodnarchuk, F. Krieg, R. Caputo, C. H. Hendon, R. X. Yang, A. Walsh and M. V. Kovalenko, *Nano Lett.*, 2015, 15, 3692-3696.
34. Y. Fu, T. Wu, J. Wang, J. Zhai, M. J. Shearer, Y. Zhao, R. J. Hamers, E. Kan, K. Deng, X. Y. Zhu and S. Jin, *Nano Lett.*, 2017, 17, 4405-4414.
35. C. Wang, A. S. R. Chesman and J. J. Jasieniak, *Chem. Commun.*, 2017, 53, 232-235.
36. U. H. Hamdeh, R. D. Nelson, B. J. Ryan, U. Bhattacharjee, J. W. Petrich and M. G. Panthani, *Chem. Mater.*, 2016, 28, 6567-6574.
37. R. L. Z. Hoye, L. C. Lee, R. C. Kurchin, T. N. Huq, K. H. L. Zhang, M. Sponseller, L. Nienhaus, R. E. Brandt, J. Jean, J. A. Polizzotti, A. Kursumović, M. G. Bawendi, V. Bulović, V. Stevanović, T. Buonassisi and J. L. MacManus-Driscoll, *Adv. Mater.*, 2017, 29, 1702176
38. R. E. Brandt, R. C. Kurchin, R. L. Z. Hoye, J. R. Poindexter, M. W. B. Wilson, S. Sulekar, F. Lenahan, P. X. T. Yen, V. Stevanović, J. C. Nino, M. G. Bawendi and T. Buonassisi, *J. Phys. Chem. Lett.*, 2015, 6, 4297.
39. B.-W. Park, B. Philippe, X. Zhang, H. Rensmo, G. Boschloo and E. M. J. Johansson, *Adv. Mater.*, 2015, 27, 6806-6813.
40. M. Leng, Z. Chen, Y. Yang, Z. Li, K. Zeng, K. Li, G. Niu, Y. He, Q. Zhou and J. Tang, *Angew. Chemie. Int. Ed.*, 2016, 55, 15012-15016.
41. B. Yang, J. Chen, F. Hong, X. Mao, K. Zheng, S. Yang, Y. Li, T. Pullerits, W. Deng, K. Han, *Angew. Chemie Int. Ed.,* 2017, 56, 12471-12475.
42. Y. Zhang, J. Yin, M. R. Parida, G. H. Ahmed, J. Pan, O. M. Bakr, J.-L. Brédas and O. F. Mohammed, *J. Phys. Chem. Lett.*, 2017, 8, 3173-3177.
43. J. Pal, S. Manna, A. Mondal, S. Das, K. V. Adarsh and A. Nag, *Angew. Chemie. Int. Ed.*, 2017, 56, 14187-14191.
44. J. Zhang, Y. Yang, H. Deng, U. Farooq, X. Yang, J. Khan, J. Tang and H. Song, *ACS Nano*, 2017, 11, 9294-9302.
45. A. Swarnkar, V. K. Ravi and A. Nag, *ACS Energy Lett.*, 2017, 2, 1089-1098.
46. K. Momma and F. Izumi, *J. Appl. Crystallogr.*, 2011, 44, 1272-1276.
47. O. Lindqvist, G. Johansson, F. Sandberg and T. Norin, *Acta Chem. Scand.*, 1968, 22, 2943-2952.
48. T. Udayabhaskararao, M. Kazes, L. Houben, H. Lin and D. Oron, *Chem. Mater.*, 2017, 29, 1302-1308.
49. A. Shavel, B. Rodríguez-González, M. Spasova, M. Farle and L. M. Liz-Marzán, *Adv. Funct. Mater.*, 2007, 17, 3870-3876.
50. N. Oh and M. Shim, *J. Am. Chem. Soc.*, 2016, 138, 10444-10451.
51. J. De Roo, M. Ibáñez, P. Geiregat, G. Nedelcu, W. Walravens, J. Maes, J. C. Martins, I. Van Driessche, M. V. Kovalenko and Z. Hens, *ACS Nano*, 2016, 10, 2071-2081.
52. Q. A. Akkerman, V. D'Innocenzo, S. Accornero, A. Scarpellini, A. Petrozza, M. Prato and L. Manna, *J. Am. Chem. Soc.*, 2015, 137, 10276-10281.
53. G. Nedelcu, L. Protesescu, S. Yakunin, M. I. Bodnarchuk, M. J. Grotevent and M. V. Kovalenko, *Nano Lett.*, 2015, 15, 5635-5640.
54. R. E. Brandt, V. Stevanović, D. S. Ginley and T. Buonassisi, *MRS Commun.*, 2015, 5, 265-275.

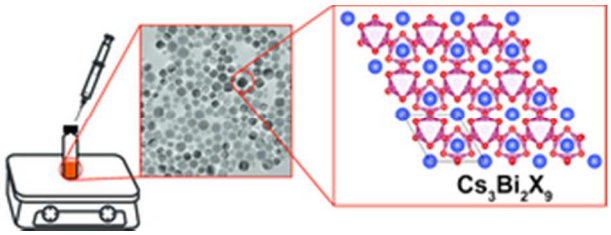

29x9mm (300 x 300 DPI)

Text to accompany abstract: 20 words or less

Vacancy-ordered cesium bismuth halide nanocrystals were synthesized using hot-injection methods.